This is a repository copy of *Sub-6 GHz channel modeling and evaluation in indoor industrial environments*.

White Rose Research Online URL for this paper:
https://eprints.whiterose.ac.uk/197794/

Version: Published Version

RESEARCH ARTICLE

Sub-6 GHz Channel Modeling and Evaluation in Indoor Industrial Environments

BERNA BULUT CEBECIOGLU[1], **YUEN KWAN MO**[1], **SON DINH-VAN**[1], **DANIEL S. FOWLER**[1],
ALEX EVANS[1], **APARAJITHAN SIVANATHAN**[2], **ERIK KAMPERT**[1,3],
BILAL AHMAD[1], (Senior Member, IEEE),
AND MATTHEW D. HIGGINS[1], (Senior Member, IEEE)

[1]Warwick Manufacturing Group (WMG), University of Warwick, CV4 7AL Coventry, U.K.
[2]AMRC North West, Roy Chadwick Way, Samlesbury Aerospace Enterprise Zone, BB2 7HP Blackburn, U.K.
[3]Institute of Fundamentals of Electrical Engineering, Helmut Schmidt University, 22043 Hamburg, Germany

Corresponding author: Berna Bulut Cebecioglu (Berna.Bulut-Cebecioglu@warwick.ac.uk)

ABSTRACT This paper presents sub-6 GHz channel measurements using a directional antenna at the transmitter and a directional or omnidirectional antenna at the receiver at 4.145 GHz in sparse and dense industrial environments for a line-of-sight scenario. Furthermore, the first measured over-the-air error vector magnitude (EVM) results depending on different 5G new radio modulation and coding schemes (MCSs of16 QAM, 64 QAM and 256 QAM) are provided. From the measurement campaigns, the path loss exponents (PLE) using a directional and an omnidirectional antenna at the receiver in the sparse and the dense environment are 1.24/1.39 and 1.35/1.5, respectively. PLE results are lower than the theoretical free space PLE of 2, indicating that indoor industrial environments have rich multipaths. The measured power delay profiles show the maximum root mean square (RMS) delay spreads of 11 ns with a directional antenna and 34 ns with an omnidirectional antenna at the receiver in a sparse industrial environment. However, in a dense industrial environment the maximum RMS delay spreads are significantly increased: maximum RMS delay spreads range from 226 to 282 ns for the omnidirectional and the directional antenna configuration. EVM measurements show that to increase coverage and enable higher MCS modes to be used for reliable data transmission, in both industrial environments using a directional antenna at the transmitter and the receiver is required. The large-scale path loss models, multipath time dispersion characteristics and EVM results provide insight into the deployments of 5G networks operating at sub-6 GHz frequency bands in different industrial environments.

INDEX TERMS 5G, channel measurement, channel modeling, channel statistics, indoor factory, industrial environment, measured EVM.

I. INTRODUCTION

With the development of information technologies, there has been a shift from traditional manufacturing to smart manufacturing. This new era is called the next industry evolution, Industry 4.0, and aims to establish a highly flexible, efficient, and cost-effective production process in manufacturing [1]. One of the driving forces for this development in manufacturing areas are the fifth generation (5G) mobile network technologies. 5G was designed to provide enhanced

The associate editor coordinating the review of this manuscript and approving it for publication was Parul Garg.

mobile broadband (eMBB), ultra-reliable and low latency communications (URLLC), and massive machine type communications (mMTC). URLLC and mMTC features provide ultra-reliable, low latency, high throughput and dependable connectivity for machine to machine (M2M) communication, industrial automation, internet of things (IOT), product/process digital twinning, etc. in smart factory scenarios. With the use of artificial intelligence, collected data can be processed and responses can be made in a timely and intelligent manner [2].

It is expected that the factories will greatly benefit from the advancements provided by 5G wireless networks. This

includes new options in the design of production processes provided via untethered machines and robots. Therefore, manufacturing companies are planning to deploy and operate their own private networks at their premises. Initially, the deployments of the private networks will be employed at sub-6 GHz frequency bands. Before a large-scale deployment of the 5G networks, extensive performance evaluations and testing are required for different industrial scenarios since industrial applications have strict latency and reliability requirements [3].

Industrial environments have been evaluated as a distinct scenario in the 3rd Generation Partnership Project (3GPP) Release 15 [4] (the scenario is called *Indoor factory* (InF)) based on wireless propagation characteristics from other indoor scenarios such as offices/shopping malls since the vast existence of highly reflective materials for RF signals such as machines, robotics, and workshops areas. In terms of propagation characteristics, metallic surfaces appear more reflective and less penetrative than ordinary building materials (e.g., concrete). Thus, understanding the propagation characteristics in industrial scenarios is pivotal for the evaluation, design, and deployment of robust wireless networks for manufacturing factories. To do that extensive channel measurements, characterisations and accurate channel models are required.

In this work, we present new wideband channel measurements and evaluation results from two different industrial environments at the 4.145 GHz frequency band for a line-of-sight (LOS) scenario using omnidirectional and directional antenna configurations, aiming to understand the channel characteristics in terms of path loss, delay spread and their effects in the received signal quality in the InF scenarios. The frequency band corresponds to 5G NR frequency range 1 (FR1) [5] and band n77 (3300 MHz – 4200 MHz), is the main focus band for the initial rollout of industrial private networks [6].

Channel measurement for indoor industrial scenarios with a carrier frequency of 4.145 GHz has not been investigated yet. Therefore, this work provides the first large-scale (path loss and shadow fading), and small-scale (root mean square (RMS) delay spread) fading modelling parameters for two typical indoor industrial scenarios namely, *sparse clutter* and *dense clutter* as defined in [4]. Further that the first measured over-the-air (OTA) error vector magnitude (EVM) results depending on different modulation and coding schemes (MCSs) defined in 5G NR [7], [8] for two scenarios and different antenna configurations (omnidirectional and directional) are presented.

The time dispersion nature of the wireless channels is generally characterised by RMS delay spread, as it is a good measure of the multipath time dispersion and coherence bandwidth nature of multipath channels, and an indication of the potential severity of inter-symbol interference (ISI). Therefore, dependencies between the RMS delay spread and EVM for different 5G NR MCS modes, antenna configurations and indoor industrial scenarios are provided. InF

channel models in the 3GPP TR 38.901 [4] rely heavily on measurement data obtained in typical propagation environments. Therefore, the measurement data provided in this paper can contribute to the 3GPP channel modelling work in [4] for indoor industrial scenarios and system-level simulations on URLLC/industrial internet of things (IIOT) applications.

The remainder of this paper is organised as follows. Section II details the related works in the literature. Section III presents the measurement scenarios, equipment setup, parameters, and procedure. Section IV and Section V provide the empirical path loss model and RMS delay spread, respectively. Measured path loss, RMS delay spread and EVM results are given in Section VI. Finally, Section VII concludes the paper.

II. RELATED WORKS

Limited works have been done on characterising the radio propagation behaviours in the InF environments, but such works will become important to understand the RF characteristics of smart factories to aid the placement of 5G-enabled sensors and IIOT equipment. In [9], narrowband channel measurements were conducted at 1300 MHz using discone antennas at the transmitter (TX) and receiver (RX) to characterise large-scale, small-scale, and temporal fading at five factories (i.e., food processing, engine manufacturing, aluminium manufacturing, casting foundry and engine machine and assembly shop). TX and RX antennas' heights were 2 m above the floor but the RX antenna height was changed to 1.5 m during height diversity experiments. Results indicated that the path loss exponent (PLE) was ranging between 1.8 and 2.8 depending on the measurement environment. Small-scale fading measurements showed a 30-35 dB dynamic fading range over distances of a few wave lengths. In [10], ultra-wideband measurements within a frequency range of 3.1-10.6 or 3.1-5.5 GHz were performed in two different industrial environments. Omnidirectional conical monopole antennas were used at the TX as well as at the RX throughout all measurement campaigns. TX antenna was elevated 3 m above ground level whereas RX remained on floor level. Results indicated that due to the multiple metallic items, the multipath environments were dense and almost all resolvable delay bins contain significant energy especially for NLOS situations at larger distances. Delay spread results ranged from 30 ns for LOS scenarios at shorter distances to 50 ns for NLOS at larger distances. In [11], directional radio channel measurements at 5.2 GHz were performed in a large car manufacturing hall and in an aircraft hangar and the analysis of the temporal, Doppler, and angular characteristics of the propagation channel were provided. Measurements were conducted by using a uniform linear array (ULA) of 8 planar antenna elements. TX was placed at 1.7 m and 5.5 m above floor level in a car manufacturing hall and an aircraft hangar, respectively. Results showed that delay spreads were in the range of 40-100 ns for LOS situations and in excess of 100 ns under NLOS situation. The work in [12] presented

the large-scale propagation characteristics for two different industrial environments, namely, open production space and dense factory clutter, at 2.3 and 5.7 GHz frequency bands using dipole antennas at the TX and RX. The measurements were performed at 24 uniformly spatial-distributed locations with a distance of 2 m to up to 34 m in each scenario considering multiple antenna configurations at 0.25 and 1.75 m heights. Results indicated that in both scenarios, the PLEs were below 2 in LOS. For NLOS, the PLEs ranged from 2.4 to 3.5.

In [13], the channel propagation parameters such as path loss exponent, RMS delay spread, number of multipath components (MPCs) and the K factor at four different frequency bands, 1.1, 1.6, 3.5, and 5.8 GHz were investigated based on the measurement data in an automobile factory. Similarly, wideband channel measurement campaigns using omnidirectional antennas at 3.7 GHz and virtual circular array antennas at 28 GHz in an industrial environment were executed in [14]. In the measurements, TX was placed at a height of 185 cm and was fixed for all measurement campaigns while the RX was positioned at 75 different positions on the floor at a height of 144 cm. For 3.7 and 28 GHz frequency bands, large-scale and small-scale parameters were provided, and the results were compared with the standardised InF model described in 3GPP TR 38.901 [4]. They concluded that the path loss characteristics were unique and highly scenario dependent.

In [15], power delay profile measurements of three different industrial indoor environments (the assembly shop, electronics room and mechanical room of an electronic manufacturing factory) were presented. The measurements were performed in the frequency range of 0.8 to 2.7 GHz using a frequency domain channel sounder and virtual antenna array technique. In these measurements, omnidirectional antennas at both TX and RX were used and they were placed at the same heights of 1.8 m above ground level. In [16], measurement campaigns were conducted at 900, 2400, and 5200 MHz implementing omnidirectional antennas of the same type at the TX and RX. TX and RX antenna heights were chosen equal to 6 m and 2 m respectively, to imitate the practical placement of industrial wireless access points and terminals. From the measurement data, large-scale fading, and temporal fading (K factor) characteristics were determined. At 2400 and 5200 MHz, the PLE was found to be lower than 2. The work in [17] presented RMS delay spread statistics from a wideband channel measurement campaign in a typical automation hall to characterise and parameterise the radio channels at a 5.85 GHz frequency band. At the TX and RX, omnidirectional antennas were used. Unlike the previous works in which the measurements were mostly performed under static environments, in [17] the measurements were performed in a real factory automation scenario where the robots were in motion and executed a typical pick-and-place process. RSM delay spreads in the weak and rich scatter environments were found to be 22.3 and 29.1 ns for LOS and 29.6 and 35.7 ns for NLOS respectively.

To characterise the RF propagation characteristics in terms of path loss and delay spread in an industrial environment (an oil rig), channel measurements were performed at 2.4 GHz and 5.8 GHz ISM bands [18]. At the TX and RX, omnidirectional antennas were implemented and mounted in stands 60 cm above the floor. PLE for LOS was found to be less than 2. The obtained PLE for 5.8 GHz band was larger than that of 2.4 GHz band. Results indicated that the RMS delay spreads increased linearly with the distance. In [19], measurements were conducted at 2.37 GHz and 5.4 GHz in five different factory halls at operational Siemens premises. RX antenna height was always set to around 2 m whereas the TX height ranged from 2 m to 8 m to cover different deployment scenarios. Measurements were conducted for different antenna configurations such as an omnidirectional array, a ULA and a uniform planar array at the TX and RX. Comprehensive channel parameters, the path loss, shadow fading, K factor, RMS delay spread, RMS angle spread, and the cross-polarisation ratio were provided for different configurations and compared with the 3GPP 38.901 indoor office results.

None of the literature works has considered the channel characterisation, modelling, and evaluation at 4.145 GHz carrier frequency for InF scenarios which is the aim of this paper.

III. MEASUREMENT SCENARIOS AND SETUP
A. MEASUREMENT SCENARIOS
In 3GPP [4], two indoor industrial scenarios namely, *sparse clutter* and *dense clutter* are defined depending on the levels of density of "clutter", e.g., machinery, assembly lines, storage shelves, etc. While *sparse clutter* scenario may include big machines composed of regular metallic surfaces such as several mixed production areas with open spaces and storage/commissioning areas, *dense clutter* may include small to medium metallic machinery and objects with irregular structures (e.g., assembly and production lines surrounded by mixed small-sized machines).

The measurements presented in this work were performed at the University of Warwick, UK in the Digital Automation Laboratory (DAL), which represents a *sparse clutter*, and the International Manufacturing Centre (IMC) Hall which represents a *dense clutter* indoor industrial scenario. Dimensions of the DAL are 29.5 m in length, 7 m in width and in 7.5 m height. As shown in Fig. 1a, there are a few big industrial machines comprised of metal or metal surfaces, open areas, and storage. The DAL is enclosed by a concrete wall on one side and glass windows on the other. The IMC Hall is densely packed with many industrial machines and some workshop areas and hence machines are surrounded by cages consisting of metal surfaces and glass windows as seen in Fig. 1b. Dimensions of the IMC Hall are 88 m length, 30 m width and 14.6 m height.

In both scenarios, the TX and the RX were mounted on the non-reflective poles as seen in Fig. 1a and Fig. 1b and
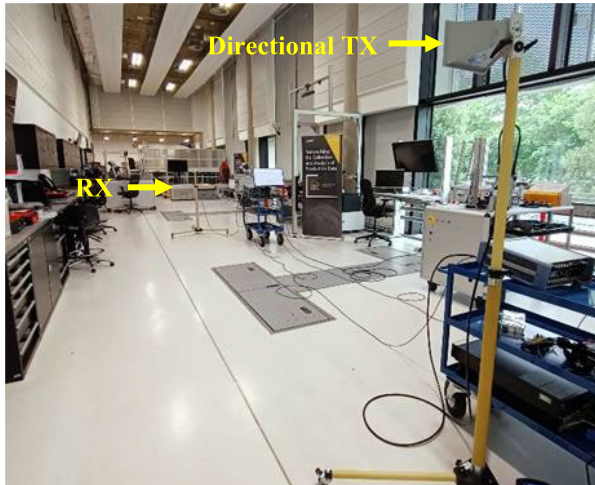
(a)   Digital Automation Laboratory (DAL)

(b)   International Manufacturing Centre (IMC) Hall

FIGURE 1. Layout of the measured indoor industrial environments (a) Digital Automation Laboratory (DAL) for sparse and (b) International Manufacturing Centre (IMC) Hall for dense.

their heights were set at 2 m and 1.5 m above the ground level respectively. The height of the RX is chosen as it is approximately the same height as for wireless terminals mounted on machinery or robot arms. On the TX side a directional antenna with 11 dBi gain was used for all measurement campaigns whereas on the RX side both directional and omnidirectional antennas with gains of 11 dBi and 3 dBi were used respectively. 5G NR is designed to operate in bands in FR1 [5] and frequency range 2 (FR2) [20]. FR1 covers the spectrum from 410MHz to 7.125 GHz whereas FR2 from 24.25 GHz to 52.6 GHz. Each frequency range is further divided into NR bands with different subcarrier spacings (SCS), channel bandwidths (BW) and duplexing modes. In this work, the carrier frequency of 4.145 GHz was used. This corresponds to our Ofcom licensed 5G NR band n77 (3300 MHz – 4200 MHz) [5]. It is worth mentioning that

during the measurements, there were no interfering wireless systems active in these frequency bands.

Further that during all measurements, the TX location was fixed, and the RX was moved to different locations to perform the measurements and to log the measured data. In DAL, the measurements were conducted with increasing TX-RX separation from 1 m to up to 15 m (maximum LOS distance) distance with an increment of 1 m, whereas in IMC the measurements were conducted from 1 m to up to 25 m with a 1 m increment. Note that during all measurements (in DAL and in IMC) the TX and RX locations had a clear optical path to one another and therefore represented a LOS environment. In addition, all channel sounding and OTA EVM measurements in DAL and IMC Hall were conducted during slow work periods to avoid exposure to external factors.

B. MEASUREMENT SETUP

In this work, the measurements were performed by using Rohde & Schwarz (R&S) time domain 5G channel sounding equipment. The channel sounding kit uses the pulse compression method and comprises a R&S SMBV100B Vector Signal Generator (VSG), and a R&S FSVA3007 Signal and Spectrum Analyzer (SSA). The VSG enables the transmission of frequency band-limited signals up to 6 GHz and an arbitrary modulated waveform with clock frequencies up to 300 MHz. The SSA enables the processing of the received signals with a maximum sampling rate of 400 MHz. The resulting I/Q data provided by the R&S FSV are evaluated by the R&S TS-5GCS Channel Sounding Software which correlates the received I/Q data with the originally transmitted sequence to calculate the channel impulse response. For indoor measurement setups, the VSG and SSA are connected via two cables which are used for synchronising the transmitter and the receiver by a reference frequency and transmitting the trigger signal.

In this work, to perform the channel sounding measurements, a 300 MHz bandwidth signal with a maximum TX power of 20 dBm was generated and transmitted with a directional TX antenna. This provided a time resolution of 3.3 ns which corresponds to a spatial resolution of 1 m. Due to its outstanding autocorrelation properties, a filtered Frank-Zadoff-Chu sequence [21] with a length of 120,000 samples was used as a channel-sounding waveform, resulting in a channel impulse response (CIR) update rate of 400 μs. In these measurements, 512 CIR values for each TX-RX location combination were automatically triggered, and the results were stored for further evaluation. Table 1 presents the parameters used in the channel-sounding measurements.

Modulation quality is defined in [8] by the difference between the measured carrier signal and the reference signal and can be represented by the error vector magnitude (EVM). Table 2 provides the EVM limits in percentage and dB depending on the MCS used. For EVM measurements, the VSG was configured based on the test models (TMs) defined in [7] and [8], i.e., based on the 5G NR Release15 downlink specifications. In this work, EVM measurements

TABLE 1. Channel sounder parameters for indoor measurements.

Parameter	Value
Carrier frequency, f_c	4.145 GHz
Bandwidth, BW	300 MHz
TX height	2 m
RX height	1.5 m
Transmit power at TX, P_t	20 dBm
Directional TX antenna gain, G_t	11 dBi
Directional RX antenna gain, G_r	11 dBi
Omnidirectional RX antenna gain, G_r	3 dBi
Cable loss, L_c	8 dB

TABLE 2. EVM limits depending on MCS Defined in [7] and [8].

MCS for PDSCH	Required EVM (%)	Required EVM (dB)
QPSK	18.5	-14.66
16 QAM	13.5	-17.39
64 QAM	9	-20.92
256 QAM	4.5	-26.94

TABLE 3. Parameters used in VSG and SSA for OTA EVM measurements.

Parameter	Value
Bandwidth, BW	100 MHz
Transmit power at TX	15 dBm
SCS	60 kHz
MCS	16 QAM, 64 QAM and 256 QAM
Duplexing	TDD

were carried out for 16 QAM, 64 QAM and 256 QAM modulation schemes (i.e., TMs) using 60 kHz SCS, 100 MHz channel BW and time division duplexing (TDD) considering the low latency requirements of the manufacturing applications. Table 3 summarises the parameters used for the OTA EVM measurements of the 5G NR signals. At the RX side (i.e., in the SSA), the same TMs and configurations were replicated to demodulate the received 5G NR signals. Carrier frequency, TX/RX heights, antennas and cables remained the same as defined in Table 1. EVM measurements were carried out at the same locations the channel sounding measurements were performed for the same antenna configurations, i.e., directional antenna at TX and omnidirectional and directional antennas at the RX. Therefore, the EVM results were obtained for directional-to-directional and directional-to-omnidirectional antenna pairs.

IV. EMPIRICAL PATH LOSS MODELS

A common path loss model is the close-in free space reference distance (CI) path loss model for a given TX-RX separation distance of dd provided in (1).

$$PL\,(d)\,[dB] = PL\,(d_0) + 10n \log_{10}\left(\frac{d}{d_0}\right) + X_\sigma\, d \geq d_0 \quad (1)$$

$$PL\,(d_0)\,[dB] = 20 \log_{10}\left(\frac{4\pi d_0}{\lambda}\right) \quad (2)$$

where d_0 is a reference distance (1 m), n is the PLE, PL (d_0) is the free space path loss at reference distance d_0 and can either be calculated from (2) with the TX and RX antenna gains included or from path loss measurements at $d_0 = 1$ m. λ is the wavelength in meters and equals to $\lambda = \frac{c}{f_c}$, where c is the speed of light in meters/s and f_c is the carrier frequency in Hertz. X_σ is a zero-mean Gaussian random variable with a standard deviation σ in dB that represents the shadow fading and is obtained by performing linear regression on the measured and estimated path loss data as [22], [23]:

$$\sigma = \sqrt{\sum_{i=1}^{N} \frac{(PL_M\,(i) - PL_E)^2}{N-1}} \quad (3)$$

where $PL_M\,(i)$ denoted measured path loss data for the ith data point, PL_E represents the estimated path loss value and N is the total number of measured path loss data points.

Regardless of the use of directional or omnidirectional antennas, the measured path loss at a distance d in meters can be calculated as a function of the transmit power P_t, TX and RX antenna gains G_t, G_r, received power P_r at the distance d and cable loss L_c (at TX and RX):

$$PL_M\,(d)\,[dB] = P_t\,[dBm] + G_t[dBi] + G_r[dBi]$$
$$- P_r\,(d)\,[dBm] - 2L_c[dB] \quad (4)$$

V. DELAY SPREAD

The time dispersion of the multipath channel provides information for the minimum symbol length to be transmitted without ISI. Therefore, the physical layer design of communication systems is often specified by the RMS delay spread and other time dispersion properties of the channels. Evaluation of such properties can provide valuable information for the design of indoor industrial communications systems. To this end, RMS delay spreads and temporal statistics for typical dense and sparse LOS industrial environments will be provided.

The RMS delay spread is calculated directly from the measured power delay profile (PDP) [22]. For each measurement, 512 CIRs and hence PDPs were captured, the received power values per delay time are then averaged over 512 CIRs to obtain one averaged PDP (APDP). Then, the RMS delay spread at each measurement location is calculated as [22]:

$$\tau_{rms} = \sqrt{\frac{\int_0^\infty (\tau - \overline{\tau})^2\, APDP(\tau)d\tau}{\int_0^\infty APDP(\tau)d\tau}} \quad (5)$$

where the mean delay $\overline{\tau}$ is given by

$$\overline{\tau} = \frac{\int_0^\infty \tau APDP(\tau)d\tau}{\int_0^\infty APDP(\tau)d\tau} \quad (6)$$

where, τ is the delay of each received MPC.

VI. RESULTS AND ANALYSIS

In the following sections, a set of new channel measurement results for two different industrial indoor scenarios at 4.145 GHz are evaluated in terms of path loss, RMS delay spread and OTA EVM. In both scenarios, measurements have been conducted for directional and omnidirectional antenna configurations at the RX while a directional antenna is always used at the TX.

A. PATH LOSS RESULTS

Fig. 2 and Fig. 3 display the path loss scatter plots and best-fit CI models (1) at 4.145 GHz in DAL and IMC Hall for omnidirectional and directional antenna configurations. In DAL, the PLEs are extracted as 1.24 and 1.39 for omnidirectional and directional antenna configurations, respectively. A similar trend, that the directional PLE is higher than the omnidirectional PLE, is observed in IMC Hall as the PLEs are found to be 1.35 and 1.5 for omnidirectional and directional antenna configurations, respectively. These results agree with the results in the literature [24]. For both antenna configurations, PLEs in IMC Hall are greater than that in DAL. As expected and seen from the results, in dense industrial environments propagation loss is higher than in sparse industrial environments. Therefore, LOS directional and omnidirectional PLEs are environment (clutter density) dependent. Furthermore, the results show that in both LOS scenarios, the PLE is below the theoretical free space PLE of 2, indicating that the propagation channel in indoor industrial environments experiences constructive interference and a waveguide effect from aisle surrounded by tall cages and machines and metallic surfaces reflections, i.e., wireless channels in industrial environments are exposed to heavy multipath propagations. The same phenomena were reported in [9], [16], and [18]. These measurement results clearly show a strong correlation between the propagation environments and the multipath channel structure even for LOS cases.
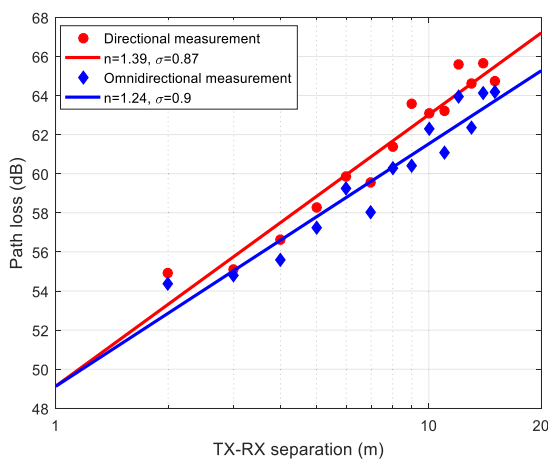

FIGURE 2. Omnidirectional and directional path loss models with the TX antenna height of 2 m and the RX antenna height of 1.5 m in a sparse industrial environment (in DAL) for a LOS scenario.
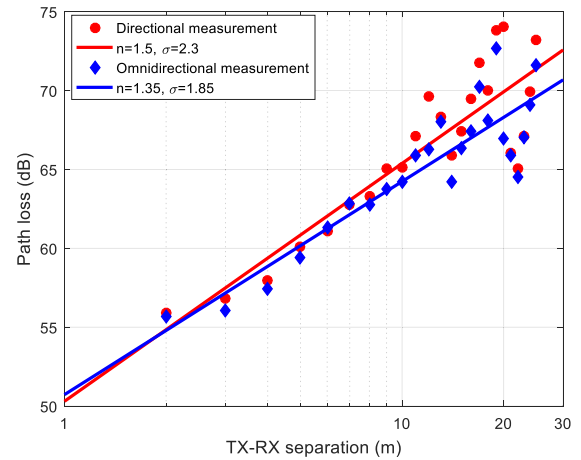

FIGURE 3. Omnidirectional and directional path loss models with the TX antenna height of 2 m and the RX antenna height of 1.5 m in a dense industrial environment (in IMC Hall) for a LOS scenario.

With respect to the shadow fading, the standard deviation (σ) values of 0.9 and 0.87 dB for the omnidirectional and directional antenna configurations in DAL, and 1.85 and 2.3 dB for the omnidirectional and directional antenna configuration in IMC Hall are observed, respectively. It is seen that the standard deviation of the shadow fading for both antenna configurations and measurements scenario are very low and close to each other. This might also be evidence for a rich scattering environment where a significant amount of MPCs decreases the shadowing effect, causing good coverage. Our results align with the literature in [19]. Further that the standard deviations show no clear dependence on the antenna configuration. However, in higher clutter density, the standard deviation is slightly increased. Comparing the standard deviation values of the shadow fading with the parameter defined in the 3GPP TR 38.901 [4] InF model for the LOS environment, the results presented in this work are lower and thus show lower signal variations around the mean.

Table 4 shows the path loss model at the reference distance $d_0 = 1$ m and the PLE, as well as the standard deviation σ for different clutter densities and antenna configurations. In this work, the path loss PL (d_0) at the reference distance $d_0 = 1$ m was calculated from the measurement. In the literature [16], it was found that using the measured path loss value at a reference distance d_0 (PL (d_0)) provided more accurate path loss modelling than using the theoretical free space path loss model at a reference distance d_0, especially as there is a height difference between the TX and the RX pair. It is shown in Table 4 that the measured path loss results (PL (d_0)) at the reference distance $d_0 = 1$ are very close. Again, there is no dependency on the antenna configuration but a slight increase (around 1-1.5 dB) is observed for the high-density environment. A similar tendency was observed in the literature [16].

B. DELAY SPREAD RESULTS

APDPs for directional and omnidirectional antennas at the distance of 15 m in DAL and IMC Hall are illustrated in

**TABLE 4.** Path loss Model Parameters with $d_0 = 1$m for 4.145 GHz industrial indoor propagation channels.

Environment	Model	PLE	σ [dB]
LOS (Directional - Omnidirectional) in DAL	$49.12 + 12.4 \log_{10}\left(\frac{d}{d_0}\right)$	1.24	0.9
LOS (Directional - Directional) in DAL	$49.13 + 13.9 \log_{10}\left(\frac{d}{d_0}\right)$	1.39	0.87
LOS (Directional - Omnidirectional) in IMC	$50.72 + 13.5 \log_{10}\left(\frac{d}{d_0}\right)$	1.35	1.85
LOS (Directional - Directional) in IMC	$50.3 + 15 \log_{10}\left(\frac{d}{d_0}\right)$	1.5	2.3

(a)   APDP in DAL (sparse)

(b)   APDP in IMC Hall (dense)

FIGURE 4. APDP at the distance of 15 m from directional and omnidirectional measurements in a LOS environment in (a) DAL (sparse) and (b) IMC Hall (dense).

Fig. 4a and Fig. 4b, respectively. From the results, a noise floor of around −110 dB is visible. Strong reflected paths are observed in the dense environment of IMC Hall for both directional and omnidirectional antennas. It is seen that the channel is not sparse and contains dense MPCs up to a delay of 2700 ns in IMC Hall. These additional periodic MPCs are from reflections from metallic sheet doors behind the TX and RX (the signal bounces between metallic sheet doors). However, in the sparse environment of DAL weak MPCs up to a maximum delay of around 900 ns are observed.

When calculating the RMS delay spread, only samples of the APDP within a certain threshold (*Thr* in dB) of the strongest path are used. In literature, it is common to use 15, 20 and 30 dB thresholds [25], [26]. In this work, *Thr* = 20dB is selected for calculating the RMS delay spreads. Fig. 5 shows the RMS delay spreads calculated from the measured APDPs depending on the distance (TX-RX separation) for the omnidirectional and the directional antenna configuration in DAL and IMC Hall, respectively. It is observed that using directional antennas at the TX and RX in a sparse environment (in DAL) reduces the time dispersion in the channel, i.e., the RMS delay spread for the directional antenna is less than 11 ns, whereas for the omnidirectional antenna it can reach up to 34 ns. However, RMS delay spread in a dense environment (in IMC Hall) depends on the objects around the TX and RX. In Fig. 1b, one side of the TX and RX is an open space, e.g., there is no metallic cages or machines nearby up to 8 m from the TX. In these locations, the RMS delay spread is lower when the directional antenna is used. Further that since the RX is close to the TX, the LOS component has much higher received power than the metallic sheet door-bounces (exceeding the 20 dB threshold). However, when the RX is surrounded by the tall metallic cages and machines (as seen in Fig. 5 from 8 m to up to 25 m) and away from the TX (in this case the received power of the LOS components gets close to the metallic sheet door-bounces), using the directional antenna causes slightly larger time dispersion than the omnidirectional one. This means that there are fewer MPCs at farther TX-RX separation distances when an omnidirectional antenna is used at the RX; this observation is more likely attributed to the noise floor in the system since MPCs become weaker as the TX-RX separation distance or propagation path distance increases. However, using a directional antenna at the RX side increases the number of detectable MPCs as well
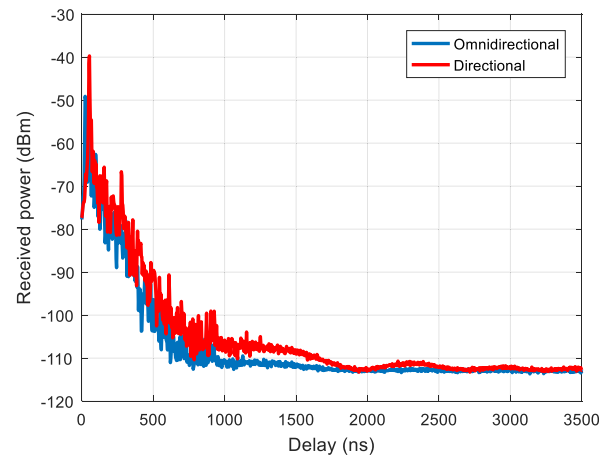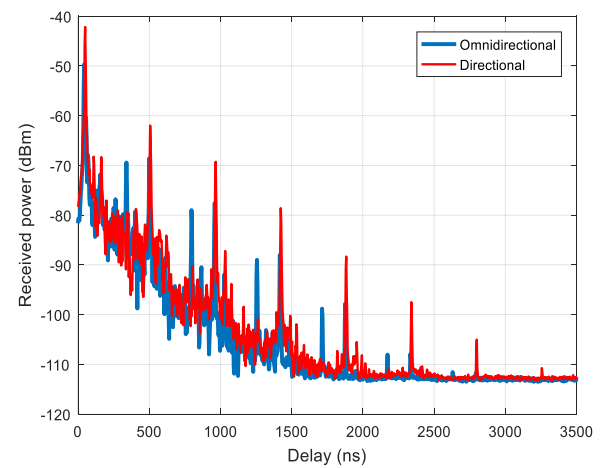
as their signal strengths which leads to higher RMS delay spreads than using the omnidirectional antenna at the RX. Similar RMS delay spread statistics at higher frequency bands (at 28, 38 and 73 GHz) were reported in [27]where the narrow beam RX antenna provided larger RMS delay spreads than the wide beam antenna.

Maximum RMS delay spreads in the dense environment (IMC Hall) are measured to be around 226 and 282 ns for the omnidirectional and the directional antenna, respectively. These increased RMS delay spreads values are attributed to the strong reflected and scattered paths received from the metallic sheet door-bounces at longer TX-RX separation distance through the 8 m to 25 m. These multipath signals tend to have large delay differences with the strongest signal, which results in large RMS delay spread values. This phenomenon is also illustrated in the APDP in Fig. 4.

Fig. 6 shows the cumulative distribution functions (CDF) for the RMS delay spreads of the APDPs measured for
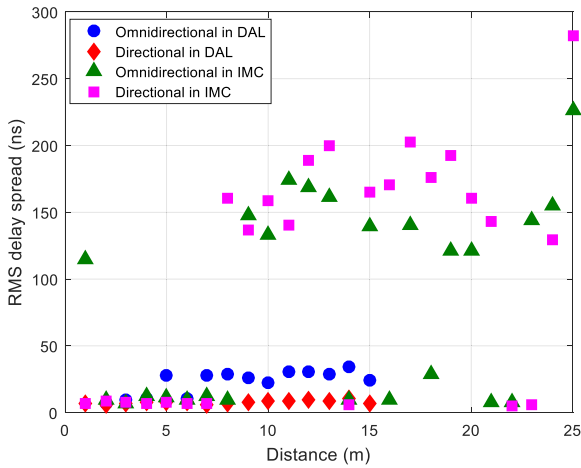
FIGURE 5. RMS delay spreads for directional and omnidirectional measurements depending on distance in a LOS environment in DAL and IMC Hall.
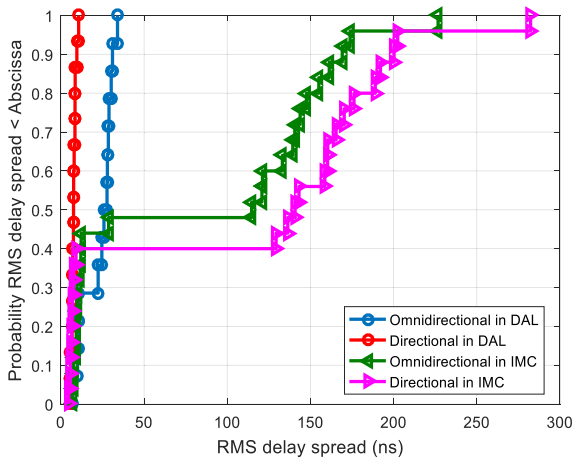
TABLE 5. Comparison of mean, standard deviation, minimum, and maximum RMS delay spreads at 4.145 GHz for directional and omnidirectional antenna configurations in LOS indoor industrial propagation environments.

Environment	μ (ns)	σ (ns)	Min. (ns)	Max. (ns)
LOS (Directional - Omnidirectional) in DAL	22	9.3	7.6	34.3
LOS (Directional - Directional) in DAL	7.6	1.4	5.6	10.6
LOS (Directional - Omnidirectional) in IMC	83.2	73.8	6.6	226.7
LOS (Directional - Directional) in IMC	106.9	88.3	4.68	282.3

FIGURE 6. CDFs of RMS delay spreads for directional and omnidirectional measurements in a LOS environment in DAL and IMC Hall.
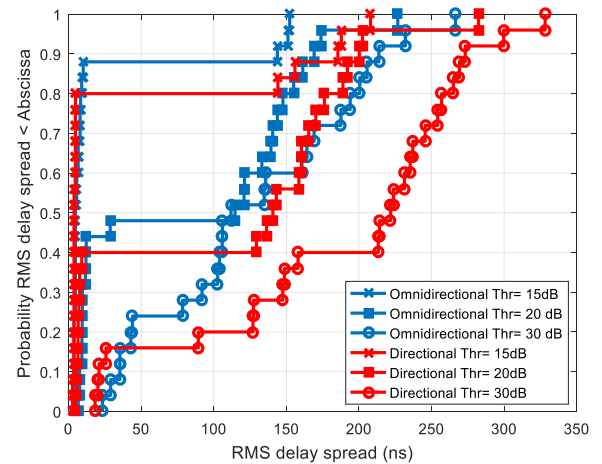

FIGURE 7. CDFs of RMS delay spreads depending on the thresholds for directional and omnidirectional measurements in a LOS environment in IMC Hall.

different antenna configurations and clutter densities. It is shown that 90% of the measured RMS delay spreads in the sparse industrial environment are less than 9 and 31 ns, whereas in the dense industrial environment they are less than 200 and 170 ns for directional, omnidirectional RX antenna configuration, respectively. It is seen that channels in the dense industrial environment have greater RMS delay spreads than the sparse industrial environment, as stated before, metallic sheet doors behind the TX and RX cause many strong reflected or scattered multipath components to arrive at the RX over a larger propagation time interval, leading to higher RMS delay spreads. Similar results were observed in propagation measurements at sub-6 GHz, conducted in [17] for indoor industrial environments.

Table 5 summarises the mean RMS delay spreads (μ in ns), the standard deviation (σ in ns), minimum, and maximum measured RMS delay spread statistics calculated for omnidirectional and directional antenna configurations in DAL and IMC Hall. We can observe that in a sparse indoor industrial

scenario (in DAL) using a directional antenna at the RX provides a much lower mean delay spread, than an omnidirectional antenna. However, in a dense indoor industrial environment (in IMC Hall), using directional antennas at the TX and RX increases the RMS delay spread since the directional antennas provide strong MPCs.

Note that the RMS delay spread statistics depend on the threshold used for data denoising. Therefore, its effect on the RMS delay spreads is further evaluated by using the measurement data collected in IMC Hall. In Fig. 7, CDFs of RMS delay spreads for different antenna configurations are compared depending on threshold levels of 15, 20, and 30 dB below the strongest ray. The results showed that when the threshold increases, the RMS delay spread increases as expected since the dynamic range is increased. Similar results were also reported in [25] and [26].

C. EVM RESULTS
The measured EVM can be used to estimate the physical layer performance of wireless communication systems as suggested in [28] since bit error rate (BER), which is used as a figure of merit for evaluating the quality of digitally modulated signals, is a direct function of the EVM, i.e., lower EVM
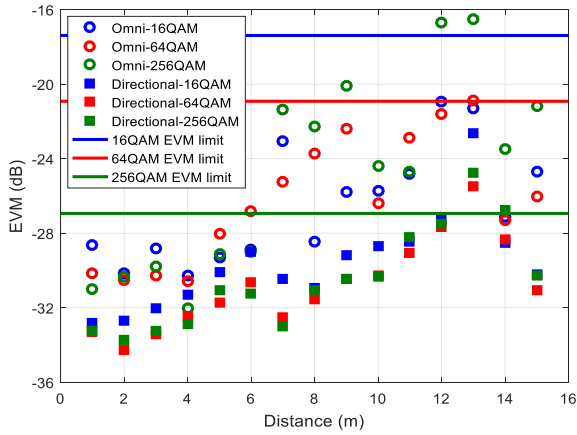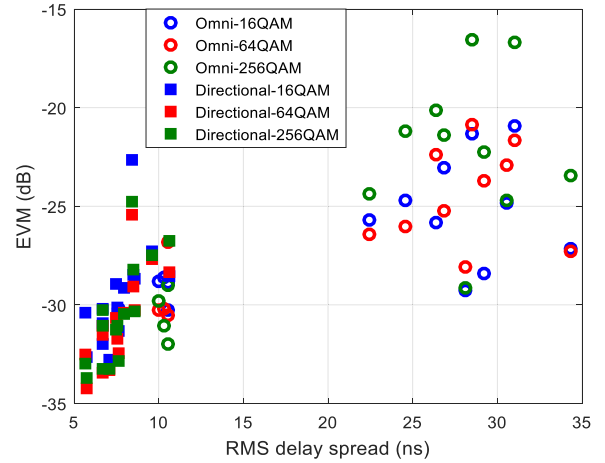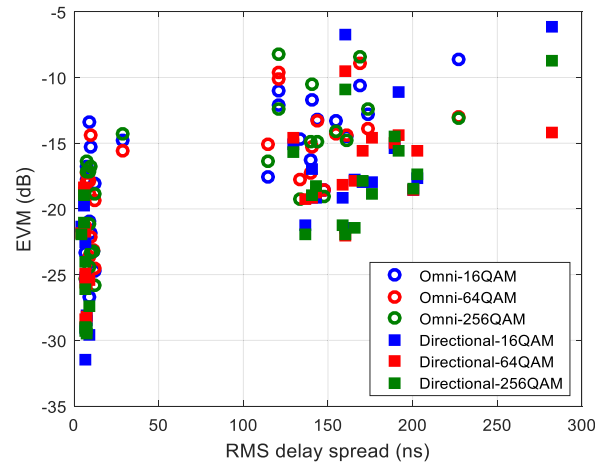
(a)   Measured EVM in DAL
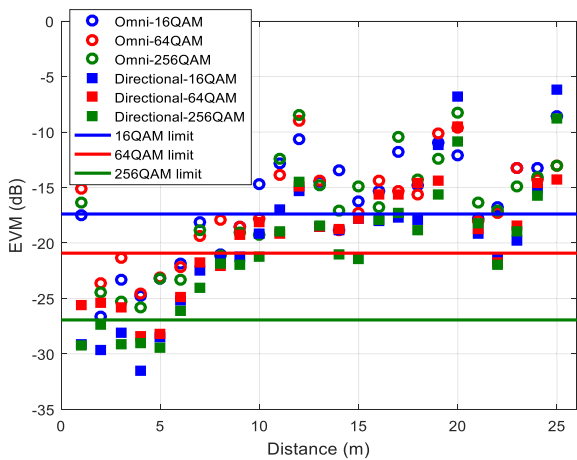
(b)   Measured EVM in IMC Hall

FIGURE 8. Measured EVM versus distance depending on the MCS mode and antenna configurations (directional and omnidirectional) for a LOS.

(a)   EVM vs. RMS delay spread in DAL

(b)   EVM vs. RMS delay spread in IMC Hall

FIGURE 9. Measured EVM versus RMS delay spread depending on the MCS mode and antenna configurations (directional and omnidirectional) for a LOS scenario in (a) DAL and (b) IMC Hall.

results in lower BER. Fig. 8a and Fig. 8b show the measured EVM versus distance depending on the 5G NR MCS modes and antenna configurations (directional and omnidirectional) for a LOS scenario in DAL and IMC Hall. As references, the required EVM values given in Table 2 are also plotted for each MCS mode. As seen in Fig. 8a, when the directional antenna is used at the RX, all MCS modes (16 QAM, 64 QAM and 256 QAM) can provide EVMs lower than the required limits thus providing a coverage range of up to 15 m in DAL. On the other hand, when the omnidirectional antenna is implemented at the RX, 16 QAM and 64 QAM can provide coverage up to 15 m but 256 QAM can only be used up to the distance of 5 m. From these results, it is clear that in a sparse industrial environment to provide reliable communications with a higher MCS such as 256 QAM it is required to use directional antennas at the TX and RX. In a dense industrial environment, the coverage ranges provided by 16 QAM, 64 QAM and 256 QAM are significantly reduced as seen in Fig. 8b, coverage ranges are 18, 8 and 5m for the directional

antenna and 9, 6 and 0 m for the omnidirectional antenna, respectively.

BER performance of wireless communication systems is a strong function of RMS delay spread [22]. Therefore, we also analyse the measured EVM results with respect to the delay spread in DAL and IMC Hall in Fig. 9a and Fig. 9b, respectively. As expected, the larger RMS delay spread results in higher EVMs thus reducing the quality and reliability of wireless systems. Similar results were noticed in [24].

VII. CONCLUSION

In this paper, the first channel sounding, and OTA EVM measurements conducted in typical sparse and dense indoor industrial environments at 4.145 GHz were presented. Large-scale path loss models and temporal statistics derived from extensive wideband measurements for omnidirectional and directional RX antennas were provided. Omnidirectional and directional path loss models as well as RMS delay spreads

and time dispersion statistics of the multipath channels were presented, yielding insight into indoor industrial propagation characteristics.

From the measurements results and analysis, it was observed that LOS PLEs for both directional and omnidirectional antennas were dependent on the environment: PLEs in DAL were 1.24 and 1.39, whereas in IMC Hall the PLE values were 1.35 and 1.5 calculated for omnidirectional and directional antenna configurations, respectively. Moreover, the results showed that in both industrial environments, constructive interference due to waveguiding and reflections resulted in the LOS PLEs lower than the theoretical free space PLE. The results demonstrated a strong correlation between the multipath distribution and the propagation environments even in LOS measurements.

Standard deviations of shadow fading were calculated as 0.9 and 0.87 dB in DAL, and 1.85 and 2.3 dB in IMC Hall for omnidirectional and directional antenna configurations, respectively. The results for both antenna configurations seemed comparable in each measurement environment. Therefore, standard deviations of shadow fading indicated no clear dependence on the antenna configuration. However, slightly higher standard deviations were observed in dense industrial environments. The standard deviation values of the shadow fading calculated in this work were lower than that defined in the 3GPP TR 38.901 InF model for the LOS environment. This was attributed to the difference in the environment and the parameters used for channel-sounding measurements.

When the time dispersion characteristics of the channels were analysed, it was found that using directional antennas at the TX and RX in the sparse environment (in DAL) reduces the time dispersion in the channel, i.e., the RMS delay spread for the directional antenna was less than 11 ns, whereas for the omnidirectional antenna it was less than 34 ns. However, in the dense environment (in IMC Hall) using the omnidirectional antenna provided lower RMS delay spread. Maximum RMS delay spreads in the dense environment were measured to be 226 and 282 ns for the omnidirectional and the directional antenna, respectively, indicating that channels in the dense industrial environment had greater RMS delay spreads than the sparse industrial environment.

The channel quality has also been investigated in terms of the measured EVM depending on the 5G NR MCS modes and antenna configurations. When the directional antenna was used at the RX, all MCS modes (16 QAM, 64 QAM and 256 QAM) met the required EVM limits thus providing a coverage range of up to 15 m. However, when the omnidirectional antenna was used at the RX, 16 QAM and 64 QAM could provide reliable communications up to the distance of 15 m but 256 QAM could only be used up to the distance of 5 m. In a dense industrial environment, the coverage ranges were significantly reduced (coverage ranges with respect MCSs of 16 QAM, 64 QAM and 256 QAM were 18, 8 and 5 m for the directional antenna and 9, 6 and 0 m for the omnidirectional antenna, respectively). Using

directional antennas at the TX and RX in both environments would provide a higher coverage range and allow higher MCS modes such as 256 QAM to be selected for data transmission thus increasing the data rate.

Lastly, the dependencies between RMS delay spread and EVM were also presented. The results show that the larger RMS delay spread led to higher EVM results and hence limited the MCS modes that could be selected for reliable data transmissions (higher MCS modes which provide higher throughput and hence lower delay would not be used).

The large-scale path loss models and multipath time dispersion characteristics presented in this work will be important for InF channel modelling and the OTA EVM results for different MCS modes may assist in the creation of new waveform designs that support 5G IIOT applications. For future work, LOS and non-LOS (NLOS) measurements with different TX and RX heights will be carried out for sub-6 GHz and millimetre wave frequencies in similar industrial environments.

REFERENCES

[1] B. Chen, J. Wan, L. Shu, P. Li, M. Mukherjee, and B. Yin, "Smart factory of industry 4.0: Key technologies, application case, and challenges," *IEEE Access*, vol. 6, pp. 6505–6519, 2017.

[2] J. Cheng, W. Chen, F. Tao, and C.-L. Lin, "Industrial IoT in 5G environment towards smart manufacturing," *J. Ind. Inf. Integr.*, vol. 10, pp. 10–19, Jun. 2018.

[3] 5G-PPP. (Oct. 2015). *White Paper on Factories-of-the-Future Vertical Sector*. [Online]. Available: https://5g-ppp.eu/wp-content/uploads/2014/02/5G-PPP-White-Paper-on-Factories-of-the-Future-Vertical-Sector.pd

[4] *Technical Specification Group Radio Access Network; Study on Channel Model for Frequencies From 0.5 to 100 GHz (Release 16)*, document TR 38.901, version 16.0.0, 3GPP, Oct. 2019.

[5] *Technical Specification Group Radio Access Network; NR; User Equipment (UE) Radio Transmission and Reception; Part 1: Range 1 Standalone (Release 17)*, document TS 38.101-1, version 17.6.0, 3GPP, Jun. 2022.

[6] *Scenarios, Frequencies and New Field Measurement Results From Two Operational Factory Halls at 3.5 GHz for Various Antenna Configurations*, document R1-1813177, 3GPP, Nokia Shanghai Bell, Spokane, WA, USA, Nov. 2018, pp. 12–16.

[7] *NR; Base Station (BS) Conformance Testing; Part 1: Conducted Conformance Testing*, document TS 38.141-.1, version 17.6.0, 3GPP, Jun. 2022.

[8] *NR; Base Station (BS) Radio Transmission and Reception (Release 17)*, document TS 38.104, version 17.6.0, 3GPP, Jun. 2022.

[9] T. S. Rappaport and C. D. McGillem, "UHF fading in factories," *IEEE J. Sel. Areas Commun.*, vol. 7, no. 1, pp. 40–48, Jan. 1989.

[10] J. Karedal, S. Wyne, P. Almers, F. Tufvesson, and A. F. Molisch, "A measurement-based statistical model for industrial ultra-wideband channels," *IEEE Trans. Wireless Commun.*, vol. 6, no. 8, pp. 3028–3037, Aug. 2007.

[11] D. Hampicke, A. Richter, A. Schneider, G. Sommerkorn, R. S. Thoma, and U. Trautwein, "Characterization of the directional mobile radio channel in industrial scenarios, based on wideband propagation measurements," in *Proc. Gateway 21st Century Commun. Village. VTC -Fall. IEEE VTS 50th Veh. Technol. Conf.*, Amsterdam, The Netherlands, Sep. 1999, pp. 2258–2262.

[12] D. A. Wassie, I. Rodriguez, G. Berardinelli, F. M. L. Tavares, T. B. Sorensen, and P. Mogensen, "Radio propagation analysis of industrial scenarios within the context of ultra-reliable communication," in *Proc. 87th Veh. Technol. Conf. (VTC-Spring)*, Jun. 2018, pp. 1–6.

[13] L. Liu, K. Zhang, C. Tao, K. Zhang, Z. Yuan, and J. Zhang, "Channel measurements and characterizations for automobile factory environments," in *Proc. 20th Int. Conf. Adv. Commun. Technol. (ICACT)*, Feb. 2018, pp. 234–238.

[14] M. Schmieder, T. Eichler, S. Wittig, M. Peter, and W. Keusgen, "Measurement and characterization of an indoor industrial environment at 3.7 and 28 GHz," in *Proc. 14th Eur. Conf. Antennas Propag. (EuCAP)*, Mar. 2020, pp. 1–5.

[15] Y. Ai, J. B. Andersen, and M. Cheffena, "Path-loss prediction for an industrial indoor environment based on room electromagnetics," *IEEE Trans. Antennas Propag.*, vol. 65, no. 7, pp. 3664–3674, Jul. 2017.

[16] E. Tanghe, W. Joseph, L. Verloock, L. Martens, H. Capoen, K. Herwegen, and W. Vantomme, "The industrial indoor channel: Large-scale and temporal fading at 900, 2400, and 5200 MHz," *IEEE Trans. Wireless Commun.*, vol. 7, no. 7, pp. 2740–2751, Jul. 2008.

[17] B. Holfeld, D. Wieruch, L. Raschkowski, T. Wirth, C. Pallasch, W. Herfs, and C. Brecher, "Radio channel characterization at 5.85 GHz for wireless M2M communication of industrial robots," in *Proc. IEEE Wireless Commun. Netw. Conf.*, Apr. 2016, pp. 1–7.

[18] S. Luo, N. Polu, Z. Chen, and J. Slipp, "RF channel modeling of a WSN testbed for industrial environment," in *Proc. IEEE Radio Wireless Symp.*, Jan. 2009, pp. 375–378.

[19] S. Jaeckel, N. Turay, L. Raschkowski, L. Thiele, R. Vuohtoniemi, M. Sonkki, V. Hovinen, F. Burkhardt, P. Karunakaran, and T. Heyn, "Industrial indoor measurements from 2–6 GHz for the 3GPP-NR and QuaDRiGa channel model," in *Proc. IEEE 90th Veh. Technol. Conf. (VTC-Fall)*, Sep. 2019, pp. 1–7.

[20] *Technical Specification Group Radio Access Network; NR; User Equipment (UE) Radio Transmission and Reception; Part 2: Range 2 Standalone (Release 17)*, document TS 38.101-2, version 17.7.0, 3GPP, Sep. 2022.

[21] R. Frank, S. Zadoff, and R. Heimiller, "Phase shift pulse codes with good periodic correlation properties (corresp.)," *IEEE Trans. Inf. Theory*, vol. IT-8, no. 6, pp. 381–382, Oct. 1962.

[22] T. S. Rappaport, *Wireless Communications: Principles and Practice*, 2nd ed. Upper Saddle River, NJ, USA: Prentice-Hall, 2002.

[23] G. R. Maccartney, T. S. Rappaport, S. Sun, and S. Deng, "Indoor office wideband millimeter-wave propagation measurements and channel models at 28 and 73 GHz for ultra-dense 5G wireless networks," *IEEE Access*, vol. 3, pp. 2388–2424, 2015.

[24] E. I. Adegoke, E. Kampert, and M. D. Higgins, "Channel modeling and over-the-air signal quality at 3.5 GHz for 5G new radio," *IEEE Access*, vol. 9, pp. 11183–11193, 2021.

[25] S. S. Ghassemzadeh, R. Jana, C. W. Rice, W. Turin, and V. Tarokh, "Measurement and modeling of an ultra-wide bandwidth indoor channel," *IEEE Trans. Commun.*, vol. 52, no. 10, pp. 1786–1796, Oct. 2004.

[26] M. Khalily, S. Taheri, S. Payami, M. Ghoraishi, and R. Tafazolli, "Indoor wideband directional millimeter wave channel measurements and analysis at 26 GHz, 32 GHz, and 39 GHz," *Trans. Emerg. Telecommun. Technol.*, vol. 29, no. 10, p. e3311, Oct. 2018.

[27] T. S. Rappaport, G. R. Maccartney, M. K. Samimi, and S. Sun, "Wideband millimeter-wave propagation measurements and channel models for future wireless communication system design," *IEEE Trans. Commun.*, vol. 63, no. 9, pp. 3029–3056, Sep. 2015.

[28] R. Shafik, M. Rahman, A. Islam, and N. Ashraf, "On the error vector magnitude as a performance metric and comparative analysis," in *Proc. Int. Conf. Emerg. Technol.*, 2006, pp. 27–31.

YUEN KWAN MO received the Ph.D. degree in communications and network engineering from the University of Warwick, Coventry, U.K. He is a Project Engineer with the Connectivity and Communications Technology Research Group, WMG, University of Warwick. His research interests include 5G and cellular communications for industry 4.0 applications, connected and autonomous vehicles, millimeter-wave communications, massive MIMO, precoding techniques, and optimization algorithms.

SON DINH-VAN received the B.S. degree from the Hanoi University of Science and Technology, Vietnam, in 2013, the M.S. degree from Soongsil University, Seoul, South Korea, in 2015, and the Ph.D. degree from the Queen's University of Belfast, Belfast, U.K., in 2019, all in electrical engineering. He was a Data Scientist with Frequenz Gmbh, Germany, and a Visiting Researcher with Middlesex University, London, U.K., in 2020 and 2021, respectively. He is currently a Research Fellow with the Connectivity and Communications Technology Research Group, WMG, University of Warwick, U.K. His current research interests include 5G-and-beyond communications for manufacturing, wireless security, millimeter-wave, and machine learning.

DANIEL S. FOWLER received the B.Eng. degree (Hons.) in computer and control system engineering, the M.S. degree in forensic computing, and the Ph.D. degree in automotive cyber security from Coventry University, U.K. He is a Research Fellow at the Secure Cyber Systems Research Group, WMG. He contributes to the open-source software community and has written over 300 articles. His research interests include secure and resilient system design. He has aided the engineering and delivery of several Innovate U.K. funded projects. He is a Chartered Engineer, and a member of IET and ACM.

BERNA BULUT CEBECIOGLU received the B.Sc. degree in electrical engineering from Kocaeli University, Kocaeli, Turkey, in 2007, the M.Sc. degree in communication networks and signal processing, and the Ph.D. degree in electrical and electronic engineering from the University of Bristol, Bristol, U.K., in 2011 and 2016, respectively. She was a Senior Research Associate in electrical and electronic engineering at the University of Bristol. She is currently a Senior Research Fellow with WMG, University of Warwick, U.K. Her research interests include 5G networks, cross-layer design and optimizations of wireless networks, multimedia multicasting and broadcasting services, propagation modeling, millimeter wave, and vehicular communications.

ALEX EVANS received the B.Sc. degree in cybernetics and control engineering from the University of Reading, in 1993. The early years of his career were spent designing, building, and programming embedded microcontroller projects for a variety of customers in scientific and automation industries. Further more than ten years working for a leading HMI Manufacturer and nine years as a Self-Employed HMI and a PLC Software Engineer enabled him to gain experience with all the leading PLC technologies, across a variety of sectors including automotive, textiles, food, utilities, building automation, and energy monitoring. He joined WMG, as a Project Engineer, in 2017, where he has been promoted to a Lead Engineer. During this time he has helped to deliver a number of industry collaborative advanced technology automation, digital manufacturing, and data collection projects.

APARAJITHAN SIVANATHAN received the M.Sc. degree in mechatronics engineering from the King's College London and the Ph.D. degree from Heriot-Watt University. He is the Head of the digital technology at the Advanced Manufacturing Research Centre North-West. He is the consortium lead for the 5G Factory of the Future Testbed program, a more than ten million projects, jointly funded by the Government and Industry, including BAE Systems and IBM. He comes from a multidisciplinary background of manufacturing, electronics, and computing. He has received prestigious research grants from DCMS, HVMC, Innovate U.K., and EPSRC Network Plus. Before entering the research career, he worked as a Research and Development Engineer in the embedded electronics industry. His current research interests include 5G for manufacturing, ultra-low latency closed loop control, real-time systems, manufacturing informatics, cyber physical spaces, and industry 4.0.

ERIK KAMPERT received the M.Sc. and Ph.D. degrees in natural sciences from Radboud University Nijmegen, The Netherlands, in 2005 and 2012, respectively. He was with the High Field Magnet Laboratory and the Molecular Materials Group, Institute for Molecules and Materials, RU. He continued his research as a Postdoctoral Researcher with the Dresden High Magnetic Field Laboratory, Helmholtz-Zentrum Dresden-Rossendorf, Germany. In 2017, he joined the Connectivity and Communications Technology Group within WMG's Intelligent Vehicles Research Team at the University of Warwick, U.K., as a Senior Research Fellow, and was promoted to an Associate Professor (Research), in 2021, focusing on 5G/6G wireless communication for the Industrial Internet of Things (IIoT) and vehicular-to-everything (V2X) applications. In 2022, he joined the Institute of Fundamentals of Electrical Engineering, Helmut Schmidt University, University of the Federal Armed Forces Hamburg, Germany. Using his vast background in RF electromagnetics, he currently investigates the electromagnetic immunity of autonomous systems as part of the Digitalization and Technology Research Center, Bundeswehr.

BILAL AHMAD (Senior Member, IEEE) received the M.Sc. degree in mechatronics and the Ph.D. degree in automation systems from Loughborough University, Loughborough, U.K., in 2007 and 2014, respectively. He was a Research Fellow and a Senior Research Fellow with WMG, University of Warwick, Coventry, U.K., and also a Research Associate at the Wolfson School of Mechanical and Manufacturing Engineering, Loughborough University. He is currently an Associate Professor with the WMG, University of Warwick. He has worked on a range of high-profile national and international research projects. He is named as a PI and a Co-I on a number of Innovate U.K. and HVM Catapult projects. He has published his research findings in over 50 peer-reviewed journal articles and conference papers. His research interests include manufacturing digitalization and lifecycle engineering of cyber–physical production systems, especially focusing on the design and deployment of real-time control systems and their connectivity with IT systems.

MATTHEW D. HIGGINS (Senior Member, IEEE) is currently a Reader with the University of Warwick, where he Leads WMG's Connectivity and Communications Technology Research Group within its Intelligent Vehicles Directorate. His research interests include span 5G and beyond, core networking, IEEE 802.3xx, GNSS, and timing, with applications to both the Automotive and Manufacturing domains. Coupled with an overarching motivation to ensure ongoing resilience of the domain is considered, he leads many high-value collaborative projects funded through EPSRC, Innovate U.K., and HVMC, and also leading multiple projects funded directly by industry.

● ● ●